doi:10.1016/S0022-2836(02)00599-5 available online at http://www.idealibrary.com on IDEAL® J. Mol. Biol. (2002) 321, 285–296

JMB

Structural Bases of Stability–function Tradeoffs in Enzymes

Beth M. Beadle and Brian K. Shoichet*

Department of Molecular Pharmacology and Biological Chemistry, Northwestern University School of Medicine 303 East Chicago Avenue S215 Chicago, IL 60611-3008, USA

The structures of enzymes reflect two tendencies that appear opposed. On one hand, they fold into compact, stable structures; on the other hand, they bind a ligand and catalyze a reaction. To be stable, enzymes fold to maximize favorable interactions, forming a tightly packed hydrophobic core, exposing hydrophilic groups, and optimizing intramolecular hydrogen-bonding. To be functional, enzymes carve out an active site for ligand binding, exposing hydrophobic surface area, clustering like charges, and providing unfulfilled hydrogen bond donors and acceptors. Using AmpC β-lactamase, an enzyme that is well-characterized structurally and mechanistically, the relationship between enzyme stability and function was investigated by substituting key active-site residues and measuring the changes in stability and activity. Substitutions of catalytic residues Ser64, Lys67, Tyr150, Asn152, and Lys315 decrease the activity of the enzyme by 10^3–10^5-fold compared to wild-type. Concomitantly, many of these substitutions increase the stability of the enzyme significantly, by up to 4.7 kcal/mol. To determine the structural origins of stabilization, the crystal structures of four mutant enzymes were determined to between 1.90 Å and 1.50 Å resolution. These structures revealed several mechanisms by which stability was increased, including mimicry of the substrate by the substituted residue (S64D), relief of steric strain (S64G), relief of electrostatic strain (K67Q), and improved polar complementarity (N152H). These results suggest that the preorganization of functionality characteristic of active sites has come at a considerable cost to enzyme stability. In proteins of unknown function, the presence of such destabilized regions may indicate the presence of a binding site.

Keywords: β-lactamase; enzyme function; enzyme stability; stability–function tradeoffs; X-ray crystal structure

*Corresponding author

Introduction

The complicated structures of enzymes reflect several competing tendencies. Among them are the balance between stability and activity. On one hand, enzymes fold into compact, stable three-dimensional structures. On the other hand, they must also be active, binding and stabilizing ligands and transition states to catalyze reactions. The structural features that confer stability appear to be opposed, or at least orthogonal, to those that confer activity.

An enzyme achieves stability through an extensive network of favorable interactions. These include the formation of a well-packed hydrophobic core surrounded by exposed hydrophilic groups, the folding of the backbone into discrete secondary structures stabilized by hydrogen bonding, and occasionally, the burial of complementary pairs of polar residues.[1] An enzyme achieves activity through a different set of structural features. In creating a site in which a ligand can bind and chemistry can occur, proteins expose hydrophobic surface area,[2] sequester charged groups from solvent,[3,4] cluster like charges,[5] provide unfulfilled hydrogen bond donors and acceptors, and promote strained conformations of residues.[6] To be available for binding and catalysis, an active site must not complement these potential opportunities with its own residues, which is exactly what happens in regions optimized for

Abbreviations used: WT, wild-type; T_m, temperature (°C) of melting; ΔH_{VH}, van't Hoff enthalpy of unfolding; ΔS_u, entropy of unfolding; ΔG_u, Gibbs free energy of unfolding; k_{cat}, catalytic rate constant; K_M, Michaelis-Menten constant.

E-mail address of the corresponding author: b-shoichet@northwestern.edu

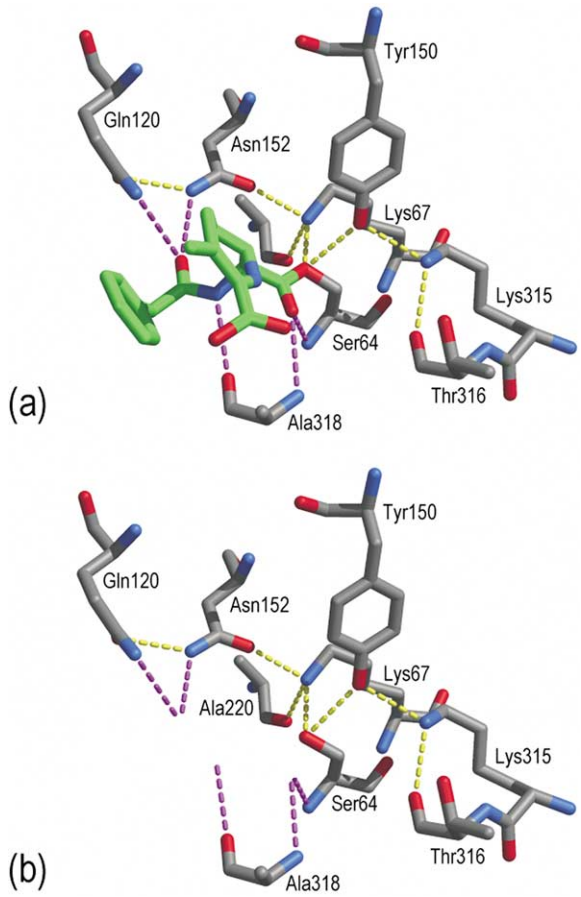

Figure 1. The active site of WT AmpC β-lactamase (PDB entry 1KE4) (a) with and (b) without ligand bound. In (a), the complex of WT AmpC with the substrate loracarbef is modeled, based on the crystal structure of loracarbef from a structure determined with a deacylation-deficient mutant enzyme (PDB entry 1FCN) modeled into the active site of the WT enzyme. Hydrogen bonds with key active-site residues are shown in purple broken lines; intra-enzyme hydrogen bonds are shown in yellow. In (b), the active site is shown without a ligand (from PDB entry 1KE4). Carbon atoms of the protein are colored gray, carbon atoms of the ligand green, oxygen atoms red, and nitrogen atoms blue. Figures 1 and 4 were generated using MidasPlus.[49]

stability. Thus, active sites appear to be regions of local instability in protein structures relative to alternate sequences.

The suggestion that active sites possess high energy, destabilizing interactions dates back to theoretical studies by Warshel;[3,4,7] presentiments of the idea may be found in work by Williams[8] and by Richards.[9] Warshel proposed that the active sites of enzymes are electrostatically preorganized to bind a transition state, fixing their dipoles and charged groups to compete with water for binding and to facilitate enzyme catalysis.[3] Whereas the dipoles of water must reorient themselves to bind a ligand, forming unfavorable interactions amongst themselves, enzymes are preformed to recognize the transition state and lower the activation barrier of the reaction.[3] Consequently, the active site of an enzyme itself is highly strained because of this preorganization.[3,4] Williams, in his discussion of the "entatic state" of proteins, also noted that metallo-enzymes often have high energy functional regions, in this case often in the metal-binding region itself. The high energy of this state can force the substrate in to a "strained" configuration to promote catalysis.[8,10] In an apparently unrelated work that nevertheless appears to speak to the same principle, Herzberg & Moult noted that strained conformations are concentrated in functional regions of protein structures.[6]

Experimental studies of the relationship between enzyme stability and function have been undertaken by several groups, most notably those of Fersht & Matthews.[1,11–13] Fersht and co-workers substituted charged active-site residues of barnase with alanine residues; the stability of the mutant enzymes was increased by as much as 0.64 kcal/mol (1 cal = 4.184 J) concomitantly, activity decreased.[11] Similar results were seen in barstar,[12] staphylococcal nuclease,[14,15] thioredoxin reductase[16] and the Cro repressor.[17] In an explicit effort to test the "stability–function" hypothesis, several functional residues of T4 lysozyme were replaced with amino acids that appeared to better complement the active site; single-residue substitutions stabilized the enzyme by up to 2 kcal/mol.[13] This led to a general formulation of the hypothesis, allowing for electrostatic preorganization of active sites, as first envisioned by Warshel, but also hydrophobic, conformational, and steric preorganization. Taken together, these results suggest that enzymes can gain significant stability from replacement of active-site residues. Conversely, little change is typically expected for randomly chosen surface substitutions on proteins,[18,19] although there are some exceptions to this trend.[20]

One limitation to previous studies is that their enzyme assays were difficult to dissect by classical kinetics. Enzymes such as lysozyme, barnase, and staphylococcal nuclease act on macromolecular ligands (e.g. cell wall, nucleic acids); it is difficult to quantify their activities rigorously. Consequently, the tradeoff between activity and stability has remained qualitative. Furthermore, most of these enzymes do not have small molecule ligands that they recognize. Because of this, it has been difficult to see if the substituted residues within the stabilized enzymes replace the normally recognized ligand functionality.

In this study, the tradeoff between stability and function is investigated quantitatively using AmpC, a class C β-lactamase. AmpC hydrolyzes β-lactams using a catalytic serine residue, Ser64. The active site appears designed to bind a β-lactam ligand, making a series of interactions between conserved residues of the enzyme and conserved moieties of the ligand (Figure 1(a)). In the absence of ligand, these interactions are largely unfulfilled; there is a large cleft, exposure of hydrophobic

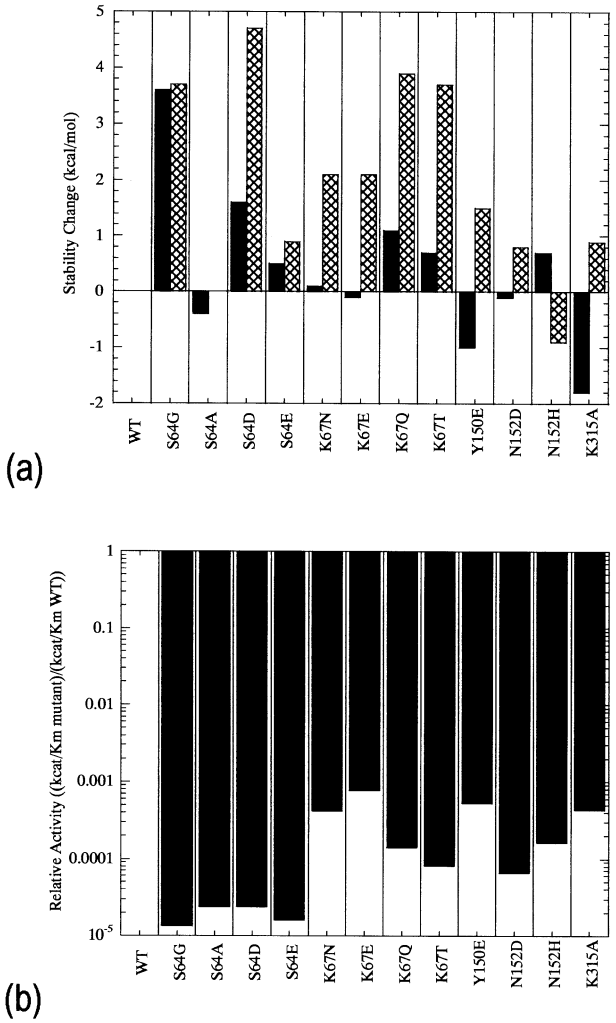

Figure 2. (a) Relative stability and (b) activity of the mutant enzymes. In (a), the change in stability (in kcal/mol) of the mutant enzymes is shown, where $\Delta\Delta G_u = \Delta G_{u,mutant} - \Delta G_{u,WT}$. Stability changes at pH 6.8 are shown in filled bars and at pH 4.4 in hatched bars. In (b), the relative activity of the mutant enzymes is shown as compared to WT. All activity measurements are at pH 7.0.

surface area, and a number of hydrogen bond acceptors and donors left without partners (Figure 1(b)). For AmpC, ligand binding produces no significant conformational changes in the key active-site residues.[21] It should be possible to stabilize the enzyme through residue substitutions in the active site that either fulfill potential interactions that the substrate is meant to make or relieve strained interactions that are thought to promote catalytic activity. For class C β-lactamases, such as AmpC, activity can be measured quantitatively by catalytic rate constant (k_{cat}) and Michaelis-Menten constant (K_M) values,[22,23] stability can be measured through reversible, two-state thermal denaturation,[24] and the structures of ligand complexes are available for many ligands.[25–29] We find by making substitutions to conserved active-site residues, namely Ser64, Lys67, Tyr150, Asn152, and Lys315, AmpC can be stabilized by up to 4.7 kcal/mol. These mutant enzymes are much reduced in catalytic activity. To investigate the source of this stability–activity tradeoff, X-ray crystal structures of four mutant enzymes were determined to between 1.90 Å and 1.50 Å resolution; they demonstrate that the enzyme can gain stability through mimicking its own ligand, forming new interactions with the protein, and by relieving strain present in the wild-type (WT) enzyme.

Results

Activity and stability of active-site mutant AmpC enzymes

Residue substitutions were made at five key positions in the active site of AmpC β-lactamase; Ser64, Lys67, Tyr150, Asn152, and Lys315. Each of these sites has been implicated in the activity of the enzyme.[25,30–33] All mutant enzymes were assayed for stability at pH 6.8 and 4.4,[24] and activity at pH 7.0 (Figure 2; Table 1).[34] Several AmpC enzymes were assayed for activity at pH 4.4. The WT enzyme was approximately fourfold less active at pH 4.4 than at pH 7.0. The mutant enzymes exhibited small differences in activity with the pH change, but all were within an order of magnitude of the activity shown at pH 7.0. Hence, all mutant enzymes had 10^3–10^5-fold less activity than the WT enzyme at both pH values.

Substitutions at the catalytic serine, Ser64, had dramatic effects on both stability and function (Figure 2; Table 1). The mutant enzymes S64G, S64D, and S64E all increased the stability of the enzyme, by up to 4.7 kcal/mol. Whereas the S64G substitution caused equivalent stability changes regardless of the pH, the S64D and S64E mutant enzymes were much more stabilized at pH 4.4. This suggests that protonation of the substituted aspartate and glutamate residues improves the complementarity for the site. Unexpectedly, S64A was actually less stable than the WT enzyme. As expected, removal of the catalytic serine residue by all substitutions dramatically decreased activity, between 42,000 and 72,000-fold, through alterations in both the k_{cat} and K_M values. These measurements may be slight overestimates of the actual activity of the mutant because of the difficulty in measuring an appreciable rate over background at high concentrations of substrate.

Substitutions at Lys67 also stabilized the enzyme (Figure 2; Table 1). K67Q and K67T were both stabilized at neutral pH. Stabilization by these two substitutions increased significantly at pH 4.4, and K67N and K67E substitutions were also stabilizing at the lower pH (Figure 2; Table 1). Activity of these mutant enzymes was decreased by 1200–12,000-fold compared to WT.

Table 1. Stability and activity measurements of AmpC mutant enzymes

	Stability at pH 6.8[a]			Stability at pH 4.4[b]			Activity[c]		
Enzyme	ΔT_m (°C)	$\Delta\Delta G_u$[d,e] (kcal/mol)	ΔH_{VH} (kcal/mol)	ΔT_m (°C)	$\Delta\Delta G_u$ (kcal/mol)	ΔH_{VH} (kcal/mol)	K_M (μM)	k_{cat} (s^{-1})	k_{cat}/K_M (s^{-1}/mM)
WT	0	0	182	0	0	172	40	200	5000
S64G	6.5	3.6	196	6.8	3.7	179	937	0.06	0.07
S64A	−0.7	−0.4	236	0	0	207	542	0.06	0.11
S64D	2.9	1.6	196	8.7	4.7	181	634	0.08	0.12
S64E	0.9	0.5	233	1.3	0.9	202	624	0.05	0.08
K67E	−0.2	−0.1	169	3.9	2.1	184	47	0.18	3.9
K67N	0.1	0.1	191	3.8	2.1	174	59	0.13	2.1
K67Q	2.0	1.1	201	7.2	3.9	202	59	0.04	0.71
K67T	1.3	0.7	193	6.9	3.7	181	65	0.03	0.41
Y150E	−1.7	−1.0	218	2.7	1.5	174	35	0.09	2.6
N152D	−0.2	−0.1	217	1.5	0.8	185	>2900	0.95	0.33
N152H	1.3	0.7	193	−1.7	−0.9	197	176	0.14	0.81
K315A	−1.8	−1.0	210	1.6	0.9	200	68	0.15	2.2
S86D[f]	0.1	0.06	205	0	0	184	ND	ND	ND
K197Q[f]	−0.3	−0.2	222	−0.1	−0.05	205	ND	ND	ND
N279H[f]	−1.0	−0.6	184	−0.5	−0.3	172	ND	ND	ND

ND, not determined.
[a] Stability at pH 6.8 was determined in a 50 mM potassium phosphate, 200 mM potassium chloride, 38% (v/v) ethylene glycol, pH 6.8 buffer.
[b] Stability at pH 4.4 was determined in a 62 mM sodium acetate, 62 mM sodium chloride, 38% (v/v) ethylene glycol, pH 4.4 buffer.
[c] Activity was determined in a 50 mM potassium phosphate, 50 mM potassium chloride, pH 7.0 buffer.
[d] Determined by the method of Schellman: $\Delta\Delta G_u = \Delta T_m \Delta S_{u,WT}$.
[e] A negative $\Delta\Delta G_u$ means a decrease in stability as indicated by a decrease in the T_m.
[f] Controls.

Substitutions at Asn152 were stabilizing for N152D and N152H (Figure 2; Table 1). The Asn → Asp substitution does not effect stability at pH 6.8 but becomes stabilizing at pH 4.4. The opposite is true for N152H; it is stabilized at pH 6.8 but becomes destabilized at pH 4.4. These results suggest that specific interactions at this position are being altered by pH changes. The activity of both mutant enzymes is decreased significantly.

A single substitution at both Lys315 and Tyr150 was stabilizing (Figure 2; Table 1). K315A and Y150E were each stabilized but only at low pH. Both of these also lost significant activity.

Stability of mutant enzymes with non-active-site surface substitutions

On the basis of the pattern of stabilization observed in the active site, three substitutions

Table 2. Crystallographic data collection and refinement statistics

	S64D	S64G	K67Q	N152H
Cell constants				
a, *b*, *c* (Å)	118.67, 76.50, 97.72	118.39, 77.33, 97.67	119.02, 76.08, 98.09	118.94, 76.26, 97.92
β (deg.)	115.65	115.76	115.84	115.69
Resolution (Å)[a]	1.53 (1.57–1.53)	1.50 (1.53–1.50)	1.90 (1.94–1.90)	1.66 (1.70–1.66)
Total observations	427,291	442,577	243,730	369,646
Unique reflections	118,322	123,526	62,018	90,254
R_{merge} (%)	6.6 (28.1)	5.3 (26.9)	7.5 (32.2)	6.0 (21.7)
Completeness (%)	99.8 (100.0)	98.8 (90.2)	99.9 (99.7)	97.0 (94.4)
$\langle I \rangle / \langle \sigma_I \rangle$	25.4 (2.7)	28.8 (2.2)	15.3 (2.3)	32.8 (5.3)
Resolution range for refinement (Å)	20–1.53	20–1.50	20–1.90	20–1.66
Number of protein residues	710	713	716	711
Number of water molecules	602	519	511	793
RMSD bond lengths (Å)	0.014	0.014	0.014	0.014
RMSD bond angles (deg.)	1.78	1.75	1.73	1.75
R-factor (%)	18.6	18.9	15.9	17.8
R_{free} (%)[b]	20.4	21.2	19.2	19.8
Average *B*-factor, protein atoms (Å^2)	20.6	21.7	20.1	17.9
Average *B*-factor, solvent atoms (Å^2)	32.8	32.4	31.1	30.5

[a] Values in parentheses are for the highest-resolution shell.
[b] R_{free} was calculated with a percentage of reflections set aside randomly: for S64D, 10%; for S64G, 2%; for K67Q, 3.5%; for N152H, 3.5%.

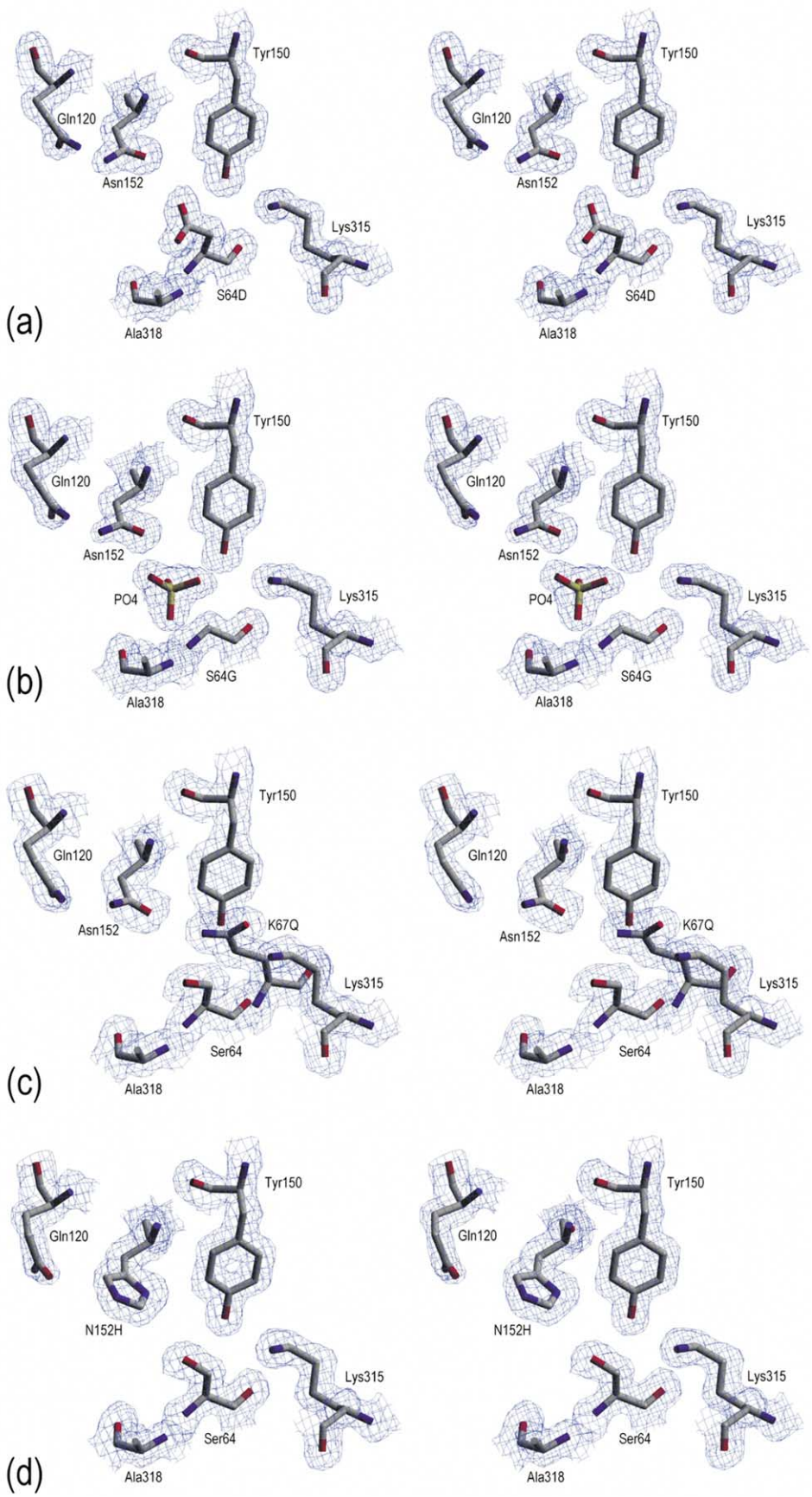

Figure 3. Stereoviews of the active site electron density for each mutant enzyme structure: (a) S64D; (b) S64G; (c) K67Q; and (d) N152H. For each, the $2F_o - F_c$ electron density of the refined model is shown in blue, contoured at 1σ. The Figure was generated using SETOR[50] and colored as in Figure 1.

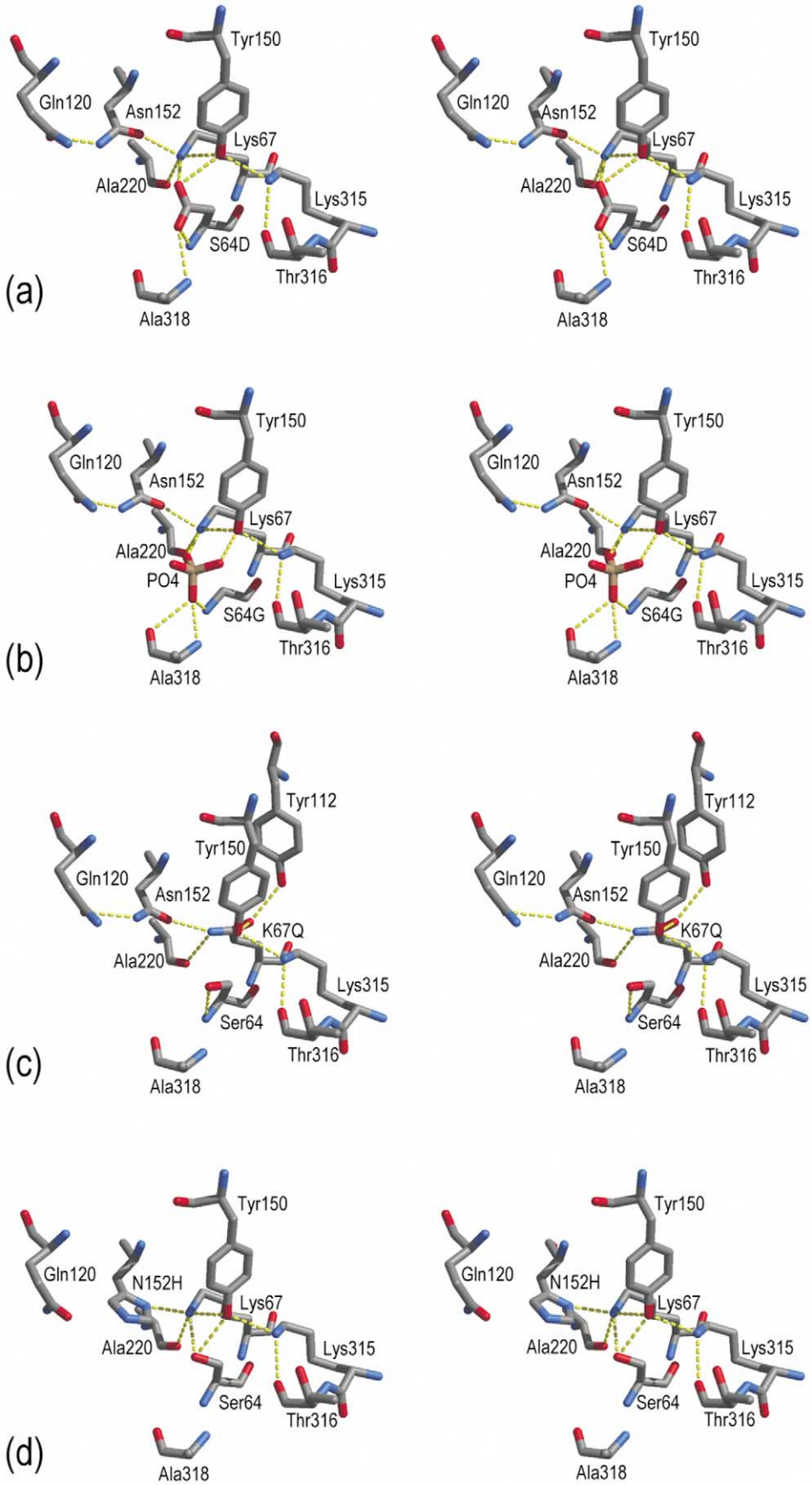

Figure 4. Stereoviews of the interactions observed within each mutant enzyme structure: (a) S64D; (b) S64G; (c) K67Q; and (d) N152H. Atoms are colored as in Figure 1. Broken yellow lines indicate hydrogen bonds.

Table 3. Key interactions within the AmpC mutant structures

Interaction	Distance (Å)				
	S64D	S64G	K67Q	N152H	WT[a]
Y150 OH-K315 N^{ζ}	2.9	2.8	3.0	2.9	2.8
Y150 OH-S64 O^{γ}	NP	NP	3.4	3.0	2.9
Y150 OH-K67 N^{ζ}	3.2	3.1	NP	3.2	3.3
K67 N^{ζ}-A220 O	2.9	2.9	NP	3.0	2.9
K67 N^{ζ}-S64 O^{γ}	NP	NP	NP	2.9	2.8
N152 $O^{\delta 1}$-K67 N^{ζ}	2.6	2.7	NP	NP	2.6
N152 $N^{\delta 2}$-Q120 $O^{\varepsilon 1}$	2.8	2.7	3.0	NP	2.8
K315 N^{ζ}-T316 O	2.9	2.8	3.1	2.8	2.8
D64 $O^{\delta 1}$-Y150 OH	2.8	NP	NP	NP	NP
D64 $O^{\delta 1}$-K67 N^{ζ}	2.9	NP	NP	NP	NP
D64 $O^{\delta 2}$-D64N	2.8	NP	NP	NP	NP
D64 $O^{\delta 2}$-A318N	3.0	NP	NP	NP	NP
D64 $O^{\delta 2}$-A318 O	3.3	NP	NP	NP	NP
Q67 $O^{\varepsilon 1}$-Y150 OH	NP	NP	3.1	NP	NP
Q67 $O^{\varepsilon 1}$-Y112 OH	NP	NP	2.9	NP	NP
Q67 $N^{\varepsilon 2}$-A220 O	NP	NP	2.9	NP	NP
Q67 $N^{\varepsilon 2}$-S64 O^{γ}	NP	NP	4.4	NP	NP
Q67 $N^{\varepsilon 2}$-N152 $O^{\delta 1}$	NP	NP	2.9	NP	NP
H152 $N^{\delta 1}$-K67 N^{ζ}	NP	NP	NP	2.7	NP

NP, not present.
[a] From PDB entry 1KE4.

were made at non-active-site surface positions; S86D, K197Q, and N279H (Table 1). These were designed as controls to compare to the same substitution made in the active site (i.e. S64D, K67Q, N152H). The sites are well-spaced around the enzyme and are solvent-exposed. For S86D and K197Q, no change in stability was observed at either pH 6.8 or pH 4.4. For N279H, the mutant enzyme was destabilized slightly (−0.6 kcal/mol at pH 6.8 and −0.3 kcal/mol at pH 4.4). Consistent with previous work,[18,19] these results suggest that non-active-site surface substitutions typically have little or, if anything, a detrimental effect on enzyme stability (we note that there are some intriguing exceptions to this general trend[20]).

X-ray crystal structures of stabilized AmpC mutant enzymes

To reveal the structural basis of the stabilization observed, X-ray crystal structures of S64D, S64G, K67Q, and N152H enzymes were determined (Table 2). In all cases, the substituted residues were modeled based on unambiguous $F_o - F_c$ electron density observed in the initial models. All models refined well, with *R*-values ranging from 15.9% to 18.9%, and R_{free} values ranging from 19.2% to 21.2% (Table 2). All models had good stereochemistry, as determined by PROCHECK;[35] for each model, 92–93% of the non-proline, non-glycine residues were in the most favored region of the Ramachandran plot, with the remainder in the additionally allowed region. For all four structures, the root-mean-squared deviation (RMSD) between monomer 2 of the mutant enzyme and monomer 2 of the WT enzyme (PDB entry 1KE4) was less than 0.14 Å.

AmpC S64D

The X-ray crystal structure of AmpC S64D was determined to 1.53 Å resolution (Table 2; Figures 3(a) and 4(a)). The substituted Asp64 makes a series of specific interactions within the active site of AmpC (Figure 4(a); Table 3). Atom $O^{\delta 1}$ of Asp64 makes interactions similar to Ser64 O^{γ} of the WT enzyme, hydrogen-bonding with Lys67 (2.9 Å) and Tyr150 (2.8 Å). The other oxygen atom, $O^{\delta 2}$, makes a new set of interactions, hydrogen-bonding with its own backbone nitrogen atom (2.8 Å), the backbone nitrogen atom of Ala318 (3.0 Å), and approaching the backbone oxygen atom of Ala318 (3.3 Å). This series of interactions resembles those seen in the complexes of β-lactams with AmpC (compare with Figure 1(a));[27,28] the O9 carbonyl oxygen atom of the β-lactam ring is recognized by these same "oxyanion"[36] or "electrophilic"[37] hole residues.

AmpC S64G

The crystal structure of AmpC S64G was determined to 1.50 Å resolution (Table 2; Figures 3(b) and 4(b)). The main-chain conformation of the active-site region is almost identical with that of the WT enzyme. However, the removal of the serine side-chain eliminates a close contact (<3.0 Å) observed between the C^{β} atom of the serine residue and the hydroxyl group of Tyr150 observed in the WT structure (PDB entry 1KE4). The substituted Gly64 allows the binding of a single phosphate ion, present in the 1.7 M crystallization buffer, in the active site of AmpC. The phosphate ion binds similarly to one seen in a high-resolution crystal structure of the WT enzyme (PDB entry 1KE4). In S64G, the phosphate ion hydrogen bonds with Lys67 (2.7 Å) and Tyr150 (3.2 Å) and residues of the oxyanion or electrophilic hole. To test whether the phosphate binding was responsible for the thermodynamic stabilization, S64G was denatured in acetate and Tris buffers; all gave the same thermodynamic values (data not shown). On the basis of the similarity between the phosphate ion positions in the WT and mutant enzyme structures, and the similar stabilization observed in the phosphate and non-phosphate buffers, we do not believe that the bound phosphate ion is responsible for the observed stabilization.

AmpC K67Q

The crystal structure of AmpC K67Q was determined to 1.90 Å resolution (Table 2; Figures 3(c) and 4(c)). Without the lysine residue at position 67, the electrostatic strain between this residue and the neighboring Lys315 has been eliminated. The substituted Gln67 increases the number of

interactions normally made at this site (Table 3). Atom $N^{\varepsilon 2}$ of Gln67 binds similarly to the Lys67 N^{ζ} atom of the WT enzyme; it interacts with Asn152 (2.9 Å) and the backbone oxygen atom of Ala220 (2.9 Å). Atom $O^{\varepsilon 1}$ of Gln67 also makes a familiar interaction, binding to Tyr150 (3.1 Å). However, this $O^{\varepsilon 1}$ atom interacts also with Tyr112 (2.9 Å), which Lys67 of the WT cannot do. The increased set of interactions is due to the greater functionality of the substituted Gln67.

AmpC N152H

The X-ray crystal structure of AmpC N152H was determined to 1.66 Å resolution (Table 2; Figures 3(d) and 4(d)). Like $O^{\delta 1}$ of the WT Asn152, N^{δ} of His152 hydrogen bonds with Lys67 (2.7 Å) (Table 3). The conformation of both the side-chain and main-chain of this residue are unaffected by the substitution.

Discussion

The two most compelling features to emerge from this study are the large increases in stability obtained from single amino acid substitutions in the active site, and the structural mechanisms conferring stabilization. At least one substitution at each active-site residue substituted stabilized the enzyme significantly, by up to 4.7 kcal/mol (Figure 2; Table 1). This is an enormous increase, given that the overall stability of the 358 residue-folded enzyme over its unfolded form ($\Delta G_u^{H_2O}$) is 14.0 kcal/mol.[24] By substituting a single active-site residue, the enzyme has increased its stability by over 30%. Concomitantly, all active-site substitutions decreased the activity of the enzyme dramatically. Similar residue substitutions at non-active-site, solvent-exposed areas of AmpC had little or no effect on stability. These results are consistent with conclusions from previous work and an analysis of the ProTherm Thermodynamic Database for Proteins and Mutants, both of which have shown that random substitutions are usually neutral with respect to stability.[18,19] This suggests that there is a tradeoff between stability and function, and that enzymes may be stabilized dramatically by active-site residue substitution.

Stabilization by substrate mimicry

Perhaps the most interesting substitutions, from a stability–function perspective, were made at Ser64, which is the catalytic, nucleophilic serine residue and is crucial for activity. In the WT enzyme, O^{γ} of Ser64 hydrogen bonds with both Lys67 and Tyr150, two residues important for activity. When replaced with glycine, aspartate, or glutamate, the stability of the enzyme is increased; however, replacement with alanine actually decreases stability.

The crystal structure of S64D explains the stabilization by the larger side-chains of aspartate and glutamate residues. The substituted Asp64 makes new interactions in the active site while maintaining those made by the WT serine residue. Because aspartate is larger than serine, the substituted $O^{\delta 2}$ of Asp64 can wrap around to bind in the oxyanion or electrophilic hole, composed of the backbone nitrogen atoms of residue 64 and Ala318, and the backbone oxygen atom of Ala318. This region is meant to recognize the O9 carbonyl oxygen atom of the β-lactam ring. In the S64D structure, the mutant residue mimics this interaction (compare Figures 4(a) and 1(a)). The mutant enzyme acts as its own ligand, stabilizing the enzyme in the same way that a β-lactam would on binding.

The interaction of the Asp64 with the oxyanion or electrophilic hole may explain the pH-dependence of stability of the S64D mutant enzyme. The differential stability of the S64D mutant enzyme, as compared to WT, increases from +1.9 kcal/mol to +4.7 kcal/mol as the pH is changed from 6.8 to 4.4. In the crystal structure, $O^{\delta 2}$ of the substituted Asp64 comes close (3.3 Å) to the backbone oxygen atom of Ala318. At pH 6.8, and also at pH 8.7 (the pH at which the crystals were grown), the substituted Asp64 would be deprotonated; this particular interaction would be unfavorable. At pH 4.4, this side-chain will be protonated, and the interaction would become favorable. This may also suggest that this region preferentially binds hydroxyl groups rather than oxyanions. Whether the oxyanion hole in serine β-lactamases is instead an electrophilic hole remains an area of active research.[37]

Stabilization by relaxation of steric strain

Unexpectedly, S64G is significantly more stable than WT, but the S64A mutant enzyme is actually less stable than WT (Figure 2). Superposition of the WT and S64G crystal structures shows that there is no change in the main-chain conformation of residue 64, which was one possible mechanism for stabilization. Another possibility is that Ser64 may be unstable because of poor electrostatic complementarity with its neighbors, which would be relieved by substitution with glycine. However, WT structures, both apo and in complex with ligands, reveal that the C^{β} atom of Ser64 is too close to Tyr150 OH (3.0 Å for WT apo), suggesting the presence of steric strain in the WT enzyme. When Ser64 is substituted with alanine, the enzyme loses the interactions made by Ser64 O^{γ} but retains the unfavorable interaction between its C^{β} atom and Tyr150. When Ser64 is truncated further to glycine, this unfavorable interaction is lost. The magnitude of the stability increase afforded by the Ser64 → Gly substitution, 3.6 kcal/mol (ΔT_m of 6.8 °C), gives an example of just how large the effects of steric strain can be in enzyme active sites.

Stabilization by relief of electrostatic strain

Various substitutions at the two active-site lysine residues, Lys67 and Lys315, resulted in significant stabilization of AmpC at pH 6.8 and even more so at pH 4.4. In the WT enzyme, Lys67 and Lys315, two conserved residues, are only 5.4 Å apart. There should be significant electrostatic strain between these two lysine residues, which are presumably protonated at both pH values. Lowering the pH would worsen the interaction of these charged residues with the rest of the protein, which would become more positively charged at pH 4.4. Hence, a more negatively charged protein (at pH 6.8) would be a better electrostatic environment for a doubly charged lysine pair than would the same protein at pH 4.4. Another possibility is that one of the lysines has a perturbed pK_a value, and it becomes positively charged only at the lower pH, increasing the electrostatic strain between the two. Regardless, replacement of either one of these lysine residues increased the stability of the enzyme, presumably by eliminating the electrostatic strain; this effect was more pronounced at the lower pH.

The crystal structure of K67Q suggests that the stabilization observed for this mutant enzyme is also, in part, due to the ability of the substituted Gln67 to make more interactions in the site (Figure 4(c)). The greater functionality of the glutamine side-chain allows the maintenance of interactions made in the WT enzyme but also gives the side-chain the opportunity to make new interactions.

Stabilization by improved polar complementarity

The substitutions at Asn152 and Tyr150 are examples of how stability can be increased through improved intramolecular interactions. In the crystal structure of N152H, the substituted His152 accepts a hydrogen bond from Lys67 (Figure 4(d)). A similar interaction occurs in the WT enzyme, but histidine is a much better base than asparagine; hence, the interaction is more favorable in the mutant enzyme. This is consistent with the pH data, which show that N152H is actually less stable than WT at low pH, where the N^{δ} of His152 would be protonated and hence unable to accept the proton from Lys67. For N152D, we hypothesize that the substituted Asp152 can maintain the same hydrogen-bonding pattern as the Asn152 when protonated; however, there are no unfulfilled hydrogen bonds with the aspartate side-chain. For these mutant enzymes, stability is increased by improved polar complementarity within the active site.

Conclusions

The active site of AmpC β-lactamase is an area of instability relative to alternate sequences, which are less functional. There are several ways that an enzyme can be stabilized by active-site residue substitutions. A stabilized mutant enzyme can mimic the ligand that it would normally recognize (as when the substituted aspartate in S64D binds in the oxyanion hole of AmpC), can eliminate strain, both electrostatic (as with substitutions at Lys67 and Lys315), and steric (as shown in S64G), and improve the complementarity within the site (as shown in N152H, among others). On the other hand, the built-in "strain" of the active site is central to its ability to recognize substrate. Much of the structure of the enzyme is devoted to ensuring that there is an oxyanion or electrophilic hole, that Lys67 and Lys315 are juxtaposed, and that Asn152 is free to donate a proton to the substrate. Here, we have tried to investigate just how large an energetic effect results from this tension between function and stability and its structural bases.

The stability–function relationship has a quality of logical necessity to it and thus suggests a method to identify active sites. If binding sites are areas of relative instability that can be stabilized, at the expense of function, then regions of the enzyme that may be stabilized by residue substitution may be binding sites. We suspect that such strained preorganization can be recognized in the active sites of most enzymes. Indeed, some groups have already begun to consider active-site stability and its relation to function.[38–40] With the structural genomics initiatives and the determination of structures of proteins of unknown function,[41,42] the ability to identify a binding site is attracting widespread attention. Here, we identify characteristics of active sites that may help to recognize them; binding sites are regions where stability rules are broken. Further, stabilizing residue substitutions may predict the type of ligand or functionality that can bind to these sites.

Materials and Methods

Enzyme mutagenesis and preparation

Mutants of AmpC were created using the overlap extension polymerase chain reaction.[43] Both WT and mutant enzymes were expressed as described.[27,37] The WT enzyme and surface-exposed control mutant enzymes (S86D, K197Q, and N279H) were purified from an *m*-aminophenylboronic acid affinity column.[37] All other mutant enzymes were purified from an S-Sepharose ion-exchange column.[27]

Enzyme stability

All enzymes were reversibly denatured by temperature in a two-state manner as described.[24] Thermal denaturations at pH 6.8 were performed in 50 mM potassium phosphate (pH 6.8), 50 mM potassium chloride, 38% (v/v) ethylene glycol buffer. Thermal denaturations at pH 4.4 were performed in a 62 mM sodium acetate (pH 4.4), 62 mM sodium chloride, 38% (v/v) ethylene glycol buffer. All T_m and ΔH_{VH} values were determined using the program EXAM[44] with a

two-state model and a ΔC_p of 6.0 kcal/mol.[24] Values of $\Delta\Delta G_u$ were calculated using the method of Schellman,[45] where $\Delta\Delta G_u = \Delta T_m \Delta S_{u,WT}$. Increases in T_m indicate stabilization, corresponding to a positive $\Delta\Delta G_u$ value.

Enzyme activity

The activity of each mutant enzyme was determined by its hydrolysis of the β-lactam substrate cephalothin (Sigma, St Louis, MO) in a 50 mM potassium phosphate, 50 mM potassium chloride buffer at pH 7.0[22] or in a 100 mM sodium acetate, 100 mM sodium chloride buffer at pH 4.4. Reaction rates were measured using a Hewlett–Packard HP-8453 spectrometer. Values of k_{cat} and K_M were determined from Lineweaver–Burk plots.

Crystallization, data collection, and data processing

Crystals of all mutant enzymes were grown by vapor diffusion in 6 μl hanging drops in 1.7 M potassium phosphate (pH 8.7).[37] X-ray diffraction data were measured at the DND-CAT beamline 5IDB at the Advanced Photon Source at Argonne National Laboratory at 100 K using a 162 mm Mar CCD detector. The HKL software suite[46] was used to index, integrate, and scale the data. All mutant enzymes crystallized in the *C*2 space group with two monomers in each asymmetric unit. All figures and interaction distances referenced are for monomer 2, which is typically better-ordered than monomer 1 and does not have a region of relative disorder from residues 280–295. Nevertheless, similar density and interactions are observed in monomer 1.

Structures were determined by molecular substitution using AmpC/boronic acid complexed structures with the residues of interest mutated to either glycine (S64G) or alanine (all others), and all solvent and inhibitor atoms removed. For S64D and S64G, the initial model was PDB entry 1C3B, and for K67Q and N152H, the initial model was PDB entry 1FSY. Each model was positioned using rigid-body refinement and then refined by simulated annealing, positional minimization, and individual *B*-factor techniques with the maximum likelihood target and a bulk solvent correction using the CNS software package.[47] For structures of S64G, K67Q, and N152H, a 2σ cutoff was applied to the data; for S64D, no σ cutoff was used. The σA-weighted electron density maps were calculated with CNS.[47] Manual rebuilding of the model and placement of water molecules was performed with the program O[48] and alternated with rounds of positional and *B*-factor refinement with CNS. For each structure, a single phosphate ion was modeled at a crystal contact. For S64G, two other phosphate ions and a sucrose molecule were included.

Protein Data Bank accession codes

The atomic coordinates and structure factors for S64D, S64G, K67Q, and N152H have been deposited in the RCSB Protein Data Bank with ID codes 1L0D, 1L0G, 1L0E, 1L0F, respectively.

Acknowledgments

This work was supported by MCB-9734484 from the NSF (to B.K.S.). B.M.B. was partly supported by NIH training grant GM08382. We thank Susan McGovern and Xiaojun Wang for reading this manuscript. We thank Rachel Powers and Pamela Focia for their assistance with crystallographic methods and manuscript revision. Crystallography data were collected at the DuPont-Northwestern-Dow Collaborative Access Team at the APS, which is supported by E. I. DuPont, deNemours & Co., the Dow Chemical Company, the NSF, and the State of Illinois.

References

1. Fersht, A. (1999). Three-dimensional structure of enzymes. In *Structure and Mechanism in Protein Science*, W. H. Freeman & Co, New York.
2. Clackson, T. & Wells, J. A. (1995). A hot spot of binding energy in a hormone-receptor interface. *Science*, **267**, 383–386.
3. Warshel, A. (1978). Energetics of enzyme catalysis. *Proc. Natl Acad. Sci. USA*, **75**, 5250–5254.
4. Warshel, A., Sussman, F. & Hwang, J. K. (1988). Evaluation of catalytic free energies in genetically modified proteins. *J. Mol. Biol.* **201**, 139–159.
5. Zhu, Z. Y. & Karlin, S. (1996). Clusters of charged residues in protein three-dimensional structures. *Proc. Natl Acad. Sci. USA*, **93**, 8350–8355.
6. Herzberg, O. & Moult, J. (1991). Analysis of the steric strain in the polypeptide backbone of protein molecules. *Proteins: Struct. Funct. Genet.* **11**, 223–229.
7. Warshel, A. (1998). Electrostatic origin of the catalytic power of enzymes and the role of preorganized active sites. *J. Biol. Chem.* **273**, 27035–27038.
8. Williams, R. J. (1972). The entatic state. *Cold Spring Harbor Symp. Quant. Biol.* **36**, 53–62.
9. Richards, F. M. (1974). The interpretation of protein structures: total volume, group volume distributions and packing density. *J. Mol. Biol.* **82**, 1–14.
10. Williams, R. J. (1995). Energised (entatic) states of groups and of secondary structures in proteins and metalloproteins. *Eur. J. Biochem.* **234**, 363–381.
11. Meiering, E. M., Serrano, L. & Fersht, A. R. (1992). Effect of active site residues in barnase on activity and stability. *J. Mol. Biol.* **225**, 585–589.
12. Schreiber, G., Buckle, A. M. & Fersht, A. R. (1994). Stability and function: two constraints in the evolution of barstar and other proteins. *Structure*, **2**, 945–951.
13. Shoichet, B. K., Baase, W. A., Kuroki, R. & Matthews, B. W. (1995). A relationship between protein stability and protein function. *Proc. Natl Acad. Sci. USA*, **92**, 452–456.
14. Hibler, D. W., Stolowich, N. J., Reynolds, M. A., Gerlt, J. A., Wilde, J. A. & Bolton, P. H. (1987). Site-directed mutants of staphylococcal nuclease. Detection and localization by ^{1}H NMR spectroscopy of conformational changes accompanying substitutions for glutamic acid-43. *Biochemistry*, **26**, 6278–6286.
15. Poole, L. B., Loveys, D. A., Hale, S. P., Gerlt, J. A., Stanczyk, S. M. & Bolton, P. H. (1991). Deletion of the omega-loop in the active site of staphylococcal nuclease. 1. Effect on catalysis and stability. *Biochemistry*, **30**, 3621–3627.
16. Gleason, F. K. (1992). Mutation of conserved residues in *Escherichia coli* thioredoxin: effects on stability and function. *Protein Sci.* **1**, 609–616.
17. Pakula, A. A. & Sauer, R. T. (1989). Amino acid substitutions that increase the thermal stability of

the lambda Cro protein. *Proteins: Struct. Funct. Genet.* **5**, 202–210.
18. Hecht, M. H., Sturtevant, J. M. & Sauer, R. T. (1984). Effect of single amino acid replacements on the thermal stability of the NH2-terminal domain of phage lambda repressor. *Proc. Natl Acad. Sci. USA*, **81**, 5685–5689.
19. Gromiha, M. M., An, J., Kono, H., Oobatake, M., Uedaira, H., Prabakaran, P. & Sarai, A. (2000). ProTherm, version 2.0: thermodynamic database for proteins and mutants. *Nucl. Acids Res.* **28**, 283–285.
20. Sanchez-Ruiz, J. M. & Makhatadze, G. I. (2001). To charge or not to charge? *Trends Biotechnol.* **19**, 132–135.
21. Beadle, B. M., Trehan, I., Focia, P. J. & Shoichet, B. K. (2002). Structural milestones in the reaction pathway of an amide hydrolase: substrate, acyl, and product complexes of cephalothin with AmpC beta-lactamase. *Structure*, **10**, 413–424.
22. Matagne, A., Misselyn-Bauduin, A. M., Joris, B., Erpicum, T., Granier, B. & Frere, J. M. (1990). The diversity of the catalytic properties of class A beta-lactamases. *Biochem. J.* **265**, 131–146.
23. Bulychev, A. & Mobashery, S. (1999). Class C beta-lactamases operate at the diffusion limit for turnover of their preferred cephalosporin substrates. *Antimicrob. Agents Chemother.* **43**, 1743–1746.
24. Beadle, B. M., McGovern, S. L., Patera, A. & Shoichet, B. K. (1999). Functional analyses of AmpC beta-lactamase through differential stability. *Protein Sci.* **8**, 1816–1824.
25. Oefner, C., D'Arcy, A., Daly, J. J., Gubernator, K., Charnas, R. L., Heinze, I. *et al.* (1990). Refined crystal structure of beta-lactamase from *Citrobacter freundii* indicates a mechanism for beta-lactam hydrolysis. *Nature*, **343**, 284–288.
26. Lobkovsky, E., Billings, E. M., Moews, P. C., Rahil, J., Pratt, R. F. & Knox, J. R. (1994). Crystallographic structure of a phosphonate derivative of the *Enterobacter cloacae* P99 cephalosporinase: mechanistic interpretation of a beta-lactamase transition-state analog. *Biochemistry*, **33**, 6762–6772.
27. Patera, A., Blaszczak, L. C. & Shoichet, B. K. (2000). Crystal structures of substrate and inhibitor complexes with AmpC beta-lactamase: possible implications for substrate-assisted catalysis. *J. Am. Chem. Soc.* **122**, 10504–10512.
28. Crichlow, G. V., Nukaga, M., Doppalapudi, V. R., Buynak, J. D. & Knox, J. R. (2001). Inhibition of class C beta-lactamases: structure of a reaction intermediate with a cephem sulfone. *Biochemistry*, **40**, 6233–6239.
29. Powers, R. A., Caselli, E., Focia, P. J., Prati, F. & Shoichet, B. K. (2001). Structures of ceftazidime and its transition-state analogue in complex with AmpC beta-lactamase: implications for resistance mutations and inhibitor design. *Biochemistry*, **40**, 9207–9214.
30. Tsukamoto, K., Tachibana, K., Yamazaki, N., Ishii, Y., Ujiie, K., Nishida, N. & Sawai, T. (1990). Role of lysine-67 in the active site of class C beta-lactamase from *Citrobacter freundii* GN346. *Eur. J. Biochem.* **188**, 15–22.
31. Monnaie, D., Dubus, A., Cooke, D., Marchand-Brynaert, J., Normark, S. & Frere, J. M. (1994). Role of residue Lys315 in the mechanism of action of the *Enterobacter cloacae* 908R beta-lactamase. *Biochemistry*, **33**, 5193–5201.
32. Dubus, A., Normark, S., Kania, M. & Page, M. G. (1995). Role of asparagine 152 in catalysis of beta-lactam hydrolysis by *Escherichia coli* AmpC beta-lactamase studied by site-directed mutagenesis. *Biochemistry*, **34**, 7757–7764.
33. Dubus, A., Ledent, P., Lamotte-Brasseur, J. & Frere, J. M. (1996). The roles of residues Tyr150, Glu272, and His314 in class C beta-lactamases. *Proteins: Struct. Funct. Genet.* **25**, 473–485.
34. Weston, G. S., Blazquez, J., Baquero, F. & Shoichet, B. K. (1998). Structure-based enhancement of boronic acid-based inhibitors of AmpC beta-lactamase. *J. Med. Chem.* **41**, 4577–4586.
35. Laskowski, R. A., MacArthur, M. W., Moss, D. S. & Thornton, J. M. (1993). PROCHECK: a program to check the stereochemical quality of protein structures. *J. Appl. Crystallog.* **26**, 283–291.
36. Murphy, B. P. & Pratt, R. F. (1988). Evidence for an oxyanion hole in serine beta-lactamases and DD-peptidases. *Biochem. J.* **256**, 669–672.
37. Usher, K. C., Blaszczak, L. C., Weston, G. S., Shoichet, B. K. & Remington, S. J. (1998). Three-dimensional structure of AmpC beta-lactamase from *Escherichia coli* bound to a transition-state analogue: possible implications for the oxyanion hypothesis and for inhibitor design. *Biochemistry*, **37**, 16082–16092.
38. Luque, I. & Freire, E. (2000). Structural stability of binding sites: consequences for binding affinity and allosteric effects. *Proteins: Struct. Funct. Genet. (Suppl)*, 63–71.
39. Elcock, A. H. (2001). Prediction of functionally important residues based solely on the computed energetics of protein structure. *J. Mol. Biol.* **312**, 885–896.
40. Ondrechen, M. J., Clifton, J. G. & Ringe, D. (2001). THEMATICS: a simple computational predictor of enzyme function from structure. *Proc. Natl Acad. Sci. USA*, **98**, 12473–12478.
41. Eisenstein, E., Gilliland, G. L., Herzberg, O., Moult, J., Orban, J., Poljak, R. J. *et al.* (2000). Biological function made crystal clear—annotation of hypothetical proteins *via* structural genomics. *Curr. Opin. Biotechnol.* **11**, 25–30.
42. Shapiro, L. & Harris, T. (2000). Finding function through structural genomics. *Curr. Opin. Biotechnol.* **11**, 31–35.
43. Ho, S. N., Hunt, H. D., Horton, R. M., Pullen, J. K. & Pease, L. R. (1989). Site-directed mutagenesis by overlap extension using the polymerase chain reaction. *Gene*, **77**, 51–59.
44. Kirchhoff, W. (1993). EXAM: A two-state thermodynamic analysis program. National Institute of Standards and Technology Technical Note 1401, National Institute of Standards and Technology, US Department of Commerce Technology Administration, Washington, DC.
45. Becktel, W. J. & Schellman, J. A. (1987). Protein stability curves. *Biopolymers*, **26**, 1859–1877.
46. Otwinowski, Z. & Minor, W. (1997). Processing of X-ray diffraction data collected in oscillation mode. *Methods Enzymol.* **276**, 307–326.
47. Brünger, A. T., Adams, P. D., Clore, G. M., DeLano, W. L., Gros, P., Grosse-Kunstleve, R. W. *et al.* (1998). Crystallography & NMR system: a new software suite for macromolecular structure determination. *Acta Crystallog. sect. D*, **54**, 905–921.
48. Jones, T. A., Zou, J. Y., Cowan, S. W. & Kjeldgaard, . (1991). Improved methods for building protein models in electron density maps and the location of errors in these models. *Acta Crystallog. sect. A*, **47**, 110–119.

49. Ferrin, T. E., Huang, C. C., Jarvis, L. E. & Langridge, R. (1988). The MIDAS display system. *J. Mol. Graph.* **6**, 13–27.

50. Evans, S. V. (1993). SETOR: hardware-lighted three-dimensional solid model representations of macromolecules. *J. Mol. Graph.* **11**, 134–138. and 127–128.

Edited by I. Wilson

(Received 14 March 2002; received in revised form 11 June 2002; accepted 13 June 2002)